

## Power Quality Improvement with Eleven Level Inverter Based Active Power Filter

V.Umamaheshwari

M.Tech Student

Sridevi Womens Engineering College.

A.Ganga Dinesh Kumar

Associate Professor

Sridevi Womens Engineering College.

### Abstract:

*The Problems due to Harmonics and responsive power losses has been relating from the decades. Since various systems are proposed to lessen those previously stated issues. One of the best methods is using 11-level inverter based dynamic active filter for the transfer of harmonics and pay of open power issues. This paper fundamentally elucidates about the new 11-level inverter based dynamic active filter advancement and different topologies utilizing as a part of the current condition, mellow procedure subsequently on for the change of power quality. Without further ado various countries has been using this MLI-AF advancement, as a consequence of its capacity to wipe out the harmonics & all the more besides size of filter is besides diminished. This new control believed is demonstrated with wide MATLAB/Simulink generation studies.*

**Key words**—Active power filter, current control, Multi level converters, predictive control.

### 1.INTRODUCTION

ELECTRIC utilities and end clients of electric force are turning out to be progressively worried about taking care of the developing vitality demand. Seventy five percent of aggregate worldwide vitality interest is supplied by the smoldering of fossil energizes. In any case, expanding air contamination, a worldwide temperature alteration concerns, decreasing fossil energizes and their expanding expense have made it important to look towards renewable sources as a future vitality arrangement. Since the previous decade, there has been a huge enthusiasm for some nations on renewable vitality for force era. The business liberalization and government's impetuses have further

quicken the renewable vitality area development. Circulated era (DG) frameworks are introduced as a suitable structure to offer high solid electrical power supply [1]. The idea is especially fascinating when various types of vitality assets are accessible, for example, photovoltaic boards, energy components, or velocity wind turbines [2], [3]. Most piece of these assets need force electronic interfaces to make up nearby air conditioning lattices [4], [5]. Thusly, inverters or air conditioning to-air conditioning converters are joined with an air conditioner basic transport with the expect to share appropriately the scatter burdens associated with the nearby lattice [6].

Most supportable vitality sources supply vitality as electrical force. Dispersed era (DG) frameworks are regularly joined with the utility framework through force electronic converters. A matrix joined inverter gives the essential interface of the DG to the stage, recurrence and sufficiency of the framework voltage, and separates the framework from the network when islanding. Such a DG framework can be intended to work in both stand-alone and matrix associated modes adaptably as indicated by network conditions [1], [2]. At the point when the utility matrix is not accessible or the utility force is incidentally lost, the DG is utilized as an on location force or standby crisis force administration, viably being an amplified uninterruptible power supply (UPS) that is fit for giving long haul vitality supply.

The non-direct load current sounds may bring about voltage music and can make a genuine PQ issue in the force framework system. Dynamic force channels (MLI-APF) are broadly used to remunerate the heap current sounds and burden unbalance at appropriation

level. This outcomes in an extra equipment cost. On the other hand, in this paper creators have joined the components of MLI-APF in the, ordinary inverter interfacing renewable with the lattice, with no extra equipment cost.

Here, the primary thought is the most extreme usage of inverter rating which is more often than not underutilized because of discontinuous nature of RES. It is indicated in this paper that the matrix interfacing inverter can adequately be used to perform taking after critical capacities: 1) exchange of dynamic force gathered from the renewable assets (wind, sunlight based, and so forth.); 2) heap receptive force interest bolster; 3) present sounds pay at PCC; and 4) present unbalance and nonpartisan current remuneration if there should arise an occurrence of 3-stage 4-wire framework. In addition, with satisfactory control of framework interfacing inverter, all the four destinations can be finished either exclusively or at the same time. The PQ requirements at the PCC can in this way be entirely kept up inside of the utility principles without extra equipment cost.

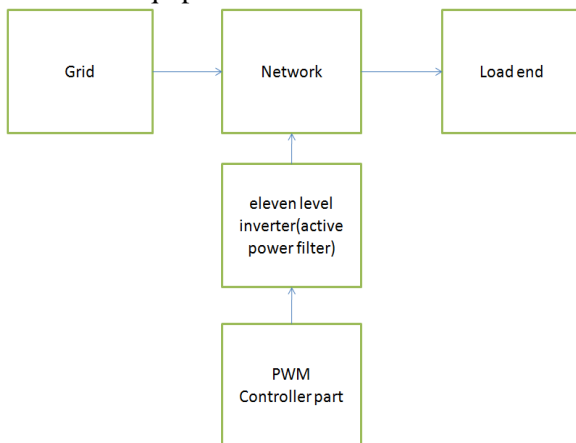


Fig 1.Proposed System Block diagram

## II. 11-LEVEL CONVERTER MODEL

By using single H-Bridge we can get 11 voltage levels. The number of output voltage levels of CHB is given by  $2n+1$  and voltage step of each level is given by  $V_{dc}/2n$ , where  $n$  is number of H-bridges connected in cascaded.

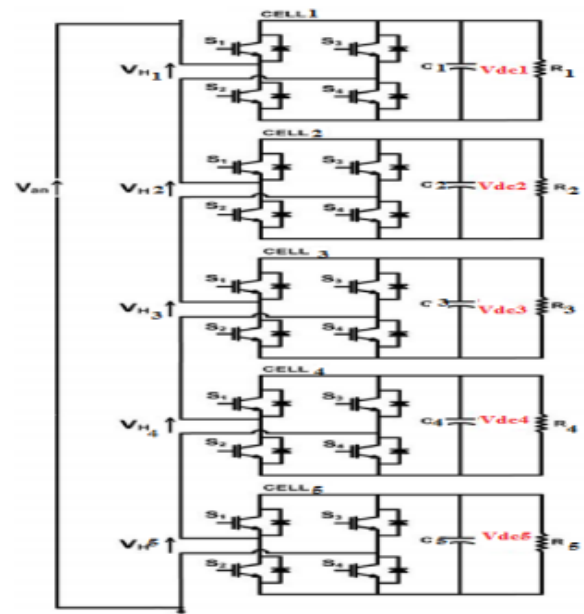


Figure-3 Single phase view of 11-level CHB inverter model

## III. DIGITAL PREDICTIVE CURRENT CONTROL

The square graph of the proposed advanced prescient current control plan is indicated in Fig. 4. This control plan is fundamentally an improvement calculation and, hence, it must be executed in a chip. Hence, the examination must be produced utilizing discrete math as a part of request to consider extra confinements, for example, time postponements and rough guesses

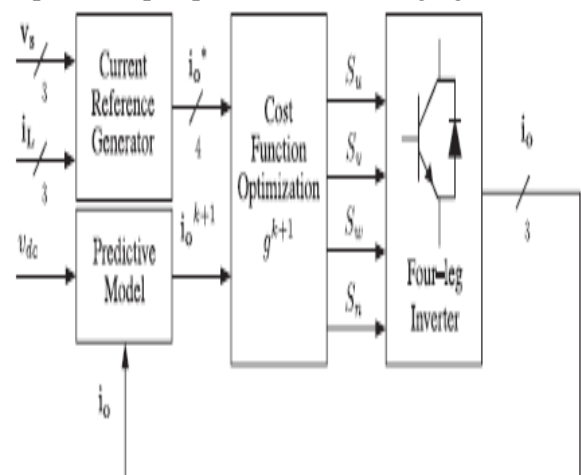


Fig. 4. Proposed predictive digital current control block diagram

[10], [22]–[27]. The primary normal for prescient control is the utilization of the framework model to foresee the future conduct of the variables to be controlled. The controller uses this data to choose the ideal exchanging express that will be connected to the force converter, as indicated by predefined enhancement criteria.

The prescient control calculation is anything but difficult to execute and to comprehend, and it can be executed with three fundamental pieces, as demonstrated in Fig. 4.

1) Current Reference Generator: This unit is intended to produce the obliged current reference that is utilized to repay the undesirable burden current segments. For this situation, the framework voltages, the heap streams, and the dc-voltage converter are measured, while the unbiased yield present and impartial burden current are created straightforwardly from these signs (IV).

2) Prediction Model: The converter model is utilized to foresee the yield converter current. Since the controller works in discrete time, both the controller and the framework model must be spoken to in a discrete time area [22]. The discrete time model comprises of a recursive framework mathematical statement that speaks to this forecast framework. This implies that for a given inspecting time  $T_s$ , knowing the converter exchanging states and control variables at moment  $kT_s$ , it is conceivable to anticipate the following states at any moment  $[k + 1]T_s$ . Due to the first-arrange nature of the state comparisons that depict the model in (1)–(2), an adequately precise first-arrange estimate of the subsidiary is considered in this paper

$$\frac{dx}{dt} \approx \frac{x[k + 1] - x[k]}{T_s} \quad (1)$$

The 16 conceivable yield current anticipated qualities can be acquired from (2) and (4) as

$$i_o[k + 1] = \frac{T_s}{L_{eq}} (v_{xn}[k] - v_o[k]) + \left(1 - \frac{R_{eq} T_s}{L_{eq}}\right) i_o[k] \quad (2)$$

As indicated in (5), with a specific end goal to anticipate the yield current  $i_o$  at the moment  $(k + 1)$ , the info voltage esteem  $v_o$  and the converter yield voltage  $v_{xN}$ , are needed. The calculation figures each of the 16 qualities connected with the conceivable mixes that the state variables can accomplish.

3) Cost Function Optimization: so as to choose the ideal exchanging express that must be connected to the force converter, the 16 anticipated qualities acquired for  $i_o[k + 1]$  are contrasted and the reference utilizing an expense capacity  $g$ , as takes after:

$$g[k + 1] = (i_{ou}^*[k + 1] - i_{ou}[k + 1])^2 + (i_{ov}^*[k + 1] - i_{ov}[k + 1])^2 + (i_{ow}^*[k + 1] - i_{ow}[k + 1])^2 + (i_{on}^*[k + 1] - i_{on}[k + 1])^2 \quad (3)$$

The yield current ( $i_o$ ) is equivalent to the reference ( $i_o^*$ ) When  $g = 0$ . Hence, the advancement objective of the expense capacity is to accomplish a  $g$  esteem near to zero. The voltage vector  $v_{xN}$  that minimizes the expense capacity is picked and afterward connected at the following inspecting state. Amid every testing express, the exchanging express that creates the base estimation of  $g$  is chosen from the 16 conceivable capacity values. The calculation chooses the exchanging express that delivers this negligible quality and applies it to the converter amid the  $k + 1$  state.

#### IV. CURRENT REFERENCE GENERATION

A dq-based current reference generator plan is utilized to acquire the dynamic force channel current reference signals. This plan shows a quick and precise sign following capacity. This trademark keeps away from voltage variances that weaken the present reference sign influencing pay execution [28]. The present reference signs are gotten from the comparing burden streams as demonstrated in Fig. 5. This module computes the reference signal streams needed by the

converter to repay responsive force, current consonant and current awkwardness. The dislodging force component ( $\sin \phi(L)$ ) and the greatest aggregate symphonious mutilation of the heap (THD(L)) characterizes the connections between the evident force needed by the dynamic force channel, as for the heap, as indicated

$$\frac{S_{APF}}{S_L} = \frac{\sqrt{\sin^2 \phi(L) + THD(L)^2}}{\sqrt{1 + THD(L)^2}} \quad (4)$$

where the estimation of THD(L) incorporates the most extreme compensable symphonious present, characterized as twofold the testing recurrence fs.

The recurrence of the greatest current consonant part that can be remunerated is equivalent to one a large portion of the converter exchanging recurrence.

The dq-based plan works in a turning reference outline; accordingly, the deliberate streams must be reproduced by the  $\sin(\omega t)$  and  $\cos(\omega t)$  signals. By utilizing dq-change, the d current part is synchronized with the relating stage to-nonpartisan framework voltage, and the q current segment is stage moved by  $90^\circ$ . The  $\sin(\omega t)$  and  $\cos(\omega t)$  synchronized reference signs are gotten from a synchronous reference outline (SRF) PLL [29]. The SRF-PLL creates an immaculate sinusoidal waveform notwithstanding when the framework voltage is seriously 690 IEEE

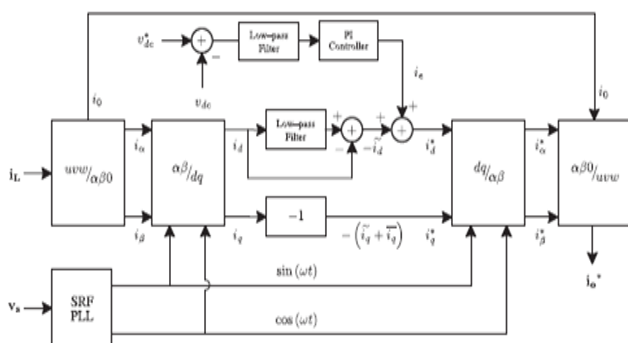


Fig. 5. DQ-Based Current Reference Generator Block Diagram.

Bended. Following mistakes are killed, subsequent to SRF-PLLs are intended to dodge stage voltage unbalancing, music (i.e., under 5% and 3% in fifth and seventh, separately), and balance brought the nonlinear weight conditions and estimation bungles [30]. Scientific explanation (8) shows the relationship between the certifiable streams  $i_{Lx}(t)$  ( $x = u, v, w$ ) and the related dq sections

$$\begin{bmatrix} i_d \\ i_q \end{bmatrix} = \sqrt{\frac{2}{3}} \begin{bmatrix} \sin \omega t & \cos \omega t \\ -\cos \omega t & \sin \omega t \end{bmatrix} \begin{bmatrix} 1 & -\frac{1}{2} & -\frac{1}{2} \\ 0 & \frac{\sqrt{3}}{2} & -\frac{\sqrt{3}}{2} \end{bmatrix} \begin{bmatrix} i_{Lu} \\ i_{Lv} \\ i_{Lw} \end{bmatrix} \quad (5)$$

A low-pass channel (LFP) removes the dc fragment of the stage streams  $i_d$  to deliver the consonant reference parts  $i_d$ .

The open reference parts of the stage streams are gotten by stage moving the relating aerating and cooling and dc sections of  $i_q$  by  $180^\circ$ . Remembering the deciding objective to keep the dc-voltage predictable, the plentifulness of the converter reference current must be changed by including a dynamic power reference hail i.e. with the d-part, as will be illuminated in Section IV-A. The consequent signs  $i^*d$  and  $i^*q$  are changed back to a three-stage structure by applying the opposite Park and Clark change, as exhibited in (9). The cutoff repeat of the LPF used as a piece of this paper is 20 Hz

$$\begin{bmatrix} i_{su}^* \\ i_{sv}^* \\ i_{sw}^* \end{bmatrix} = \sqrt{\frac{2}{3}} \begin{bmatrix} \frac{1}{\sqrt{2}} & 1 & 0 \\ \frac{1}{\sqrt{2}} & -\frac{1}{2} & \frac{\sqrt{3}}{2} \\ \frac{1}{\sqrt{2}} & -\frac{1}{2} & -\frac{\sqrt{3}}{2} \end{bmatrix} \times \begin{bmatrix} 1 & 0 & 0 \\ 0 & \sin \omega t & -\cos \omega t \\ 0 & \cos \omega t & \sin \omega t \end{bmatrix} \begin{bmatrix} i_o \\ i_d^* \\ i_q^* \end{bmatrix} \quad (6)$$

The present that travels through the neutral of the stack is reimbursed by implanting the same quick quality procured

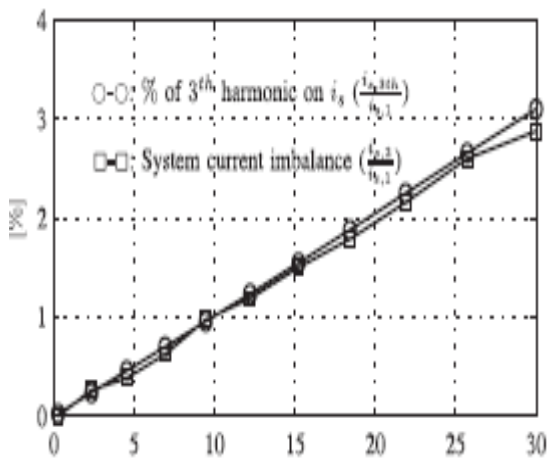


Fig. 6. Relationship between permissible unbalance load currents, the corresponding third-order harmonic content, and system current imbalance (with respect to positive sequence of the system current,  $i_{s,1}$  ).

From the stage streams, stage moved by 180°, as showed next

$$i^*_{on} = -(iL_u + iL_v + iL_w) \quad (7)$$

One of the critical central purposes of the dq-based current reference generator arrangement is that it allows the execution of an immediate controller in the dc-voltage control circle. On the other hand, one basic damage of the dq-based current reference layout figuring used to make the present reference is that a second demand symphonious part is created in  $i_d$  and  $i_q$  under unequal working conditions. The a abundance of this symphonious depends on upon the percent of uneven weight current (conveyed as the relationship between the negative gathering current  $iL_2$  and the positive plan current  $iL_1$  ). The second-organize symphonious can't be removed from  $i_d$  and  $i_q$  , and in this way delivers a third consonant in the reference current when it is changed over back to abc layout [31]. Fig. 6 exhibits the percent of structure current unevenness and the percent of third symphonious system current, in limit of the percent of weight current ponderousness. Since the stack current does not have a third consonant, the one delivered by the dynamic power channel streams to the power structure.

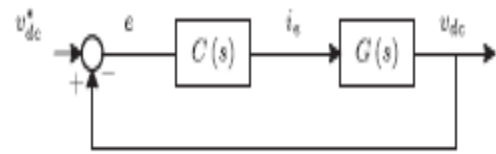


Fig. 7. DC-voltage control block diagram.

### A. DC-Voltage Control

The dc-voltage converter is controlled with a traditional PI controller. This is a discriminating issue in the evaluation, since the cost work (6) is arranged using simply current references, remembering the finished objective to keep up a vital separation from the use of weighting components. Overall, these weighting variables are gotten probably, and they are not all around described when particular working conditions are required.

Likewise, the moderate component response of the voltage over the electrolytic capacitor does not impact the present transient response. Thusly, the PI controller identifies with an essential and convincing alternative for the dc-voltage control. The dc-voltage stays steady (with a base estimation of 6 vs(rms) ) until the dynamic power devoured by the converter decreases to a level where it is not ready to conform for its mishaps. The dynamic power devoured by the converter is controlled by changing the plentifulness of the dynamic power reference hail  $i_e$  , which is in stage with each stage voltage. In the square diagram demonstrated in Fig. 5, the dc-voltage  $v_{dc}$  is measured and after that differentiated and a predictable reference regard  $v^*_{dc}$ . The misstep ( $e$ ) is taken care of by a PI controller, with two augmentations,  $K_p$  and  $T_i$ .

Both increments are processed by component response essential. Fig. 7 exhibits that the yield of the PI controller is supported to the dc-voltage trade limit  $G_s$  , which is addressed by a first-organize structure (11)

$$G(s) = \frac{v_{dc}}{i_e} = \frac{3 K_p v_s \sqrt{2}}{2 C_{dc} v^*_{dc}} \quad (8)$$

The proportionate close circle trade limit of the given system with a PI controller (12) is exhibited in (13)

$$C(s) = K_p \left( 1 + \frac{1}{T_i \cdot s} \right) \quad (9)$$

$$\frac{v_{dc}}{i_e} = \frac{\frac{\omega_n^2}{a} \cdot (s + a)}{s^2 + 2\zeta\omega_n \cdot s + \omega_n^2} \quad (10)$$

Since the time response of the dc-voltage control circle does not ought to be brisk, a damping component  $\zeta = 1$  and a trademark exact rate  $\omega_n = 2\pi \cdot 100$  rad/s are used to get a discriminatingly damped response with immaterial voltage influencing. The relating fundamental time  $T_i = 1/a$  (13) and relative expansion  $K_p$  can be

$$\zeta = \sqrt{\frac{3 K_p v_s \sqrt{2} T_i}{8 C_{dc} v_{dc}^*}} \quad (11)$$

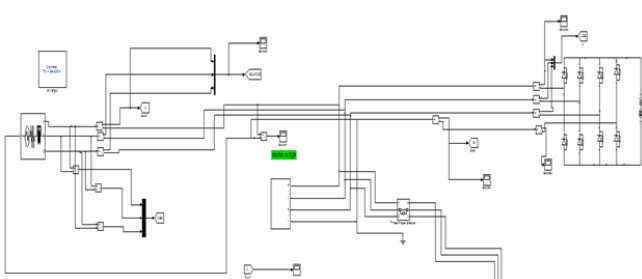
$$\omega_n = \sqrt{\frac{3 K_p v_s \sqrt{2}}{2 C_{dc} v_{dc}^* T_i}} \quad (12)$$

### V. SIMULATION RESULTS

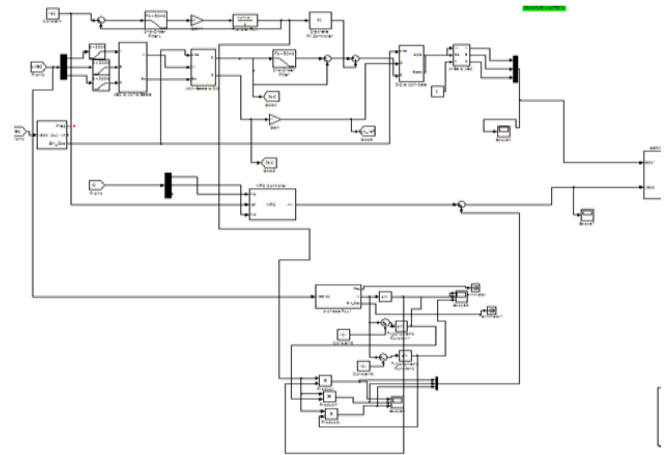
Simulation is performed using MATLAB/SIMULINK software. Simulink library files include inbuilt models of many electrical and electronics components and devices such as diodes, MOSFETS, capacitors, inductors, motors, power supplies and so on. The circuit components are connected as per design without error, parameters of all components are configured as per requirement and simulation is performed.

#### Simulation Circuit

##### a) Power circuit

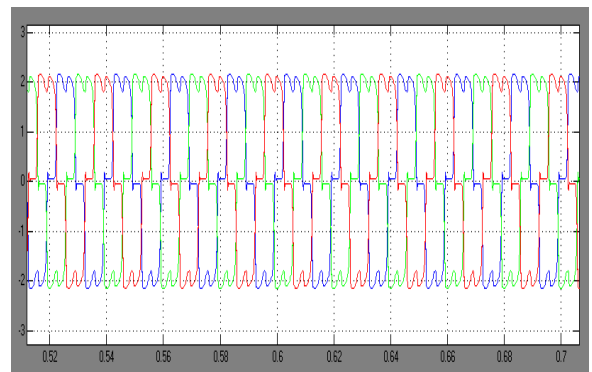


##### b) Control circuit

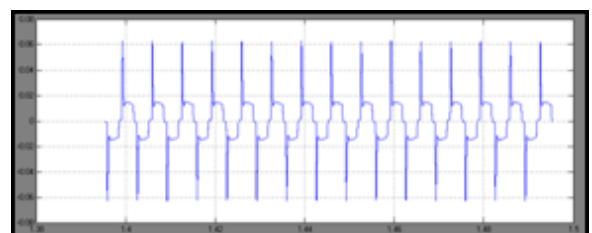


#### Waveforms

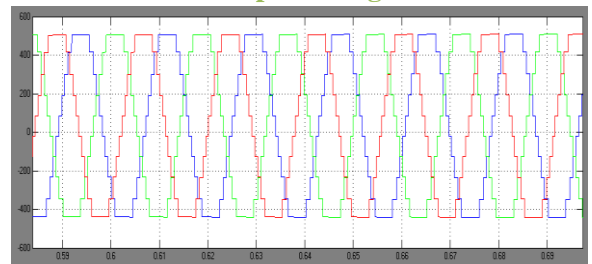
##### a) SOURCE current



##### b) Neutral current



##### c) 11-level inverter output voltages



## VI. CONCLUSION

This paper presents about the new 11-level inverter based dynamic active filter. This MLI-AF advancement, as a consequence of its capacity to wipe out the harmonics & all the more besides size of filter is besides diminished. A predictive control algorithm is designed to operate it. This new control believed is demonstrated with wide MATLAB/ Simulink generation studies.

## REFERENCES

- [1] S. Ali, M. Kazmierkowski, "PWM voltage and current control of four-leg VSI," presented at the ISIE, Pretoria, South Africa, vol. 1, pp. 196–201, Jul. 1998
- [2] S. Kouro, P. Cortes, R. Vargas, U. Ammann, and J. Rodriguez, "Model predictive control—A simple and powerful method to control power converters," IEEE Trans. Ind. Electron., vol. 56, no. 6, pp. 1826–1838, Jun. 2009.
- [3] D. Quevedo, R. Aguilera, M. Perez, P. Cortes, and R. Lizana, "Model predictive control of an AFE rectifier with dynamic references," IEEE Trans. Power Electron., vol. 27, no. 7, pp. 3128–3136, Jul. 2012.
- [4] Z. Shen, X. Chang, W. Wang, X. Tan, N. Yan, and H. Min, "Predictive digital current control of single-inductor multiple-output converters in CCM with low cross regulation," IEEE Trans. Power Electron., vol. 27, no. 4, pp. 1917–1925, Apr. 2012.
- [5] M. Rivera, C. Rojas, J. Rodriidguez, P. Wheeler, B. Wu, and J. Espinoza, "Predictive current control with input filter resonance mitigation for a direct matrix converter," IEEE Trans. Power Electron., vol. 26, no. 10, pp. 2794–2803, Oct. 2011.
- [6] M. Preindl and S. Bolognani, "Model predictive direct speed control with finite control set of PMSM drive systems," IEEE Trans. Power Electron., 2012.
- [7] T. Geyer, "Computationally efficient model predictive direct torque control," IEEE Trans. Power Electron., vol. 26, no. 10, pp. 2804–2816, Oct. 2011.
- [8] M. I. M. Montero, E. R. Cadaval, and F. B. Gonzalez, "Comparison of control strategies for shunt active power filters in three-phase four-wire systems," IEEE Trans. Power Electron., vol. 22, no. 1, pp. 229–236, Jan. 2007.
- [9] S.-K. Chung, "A phase tracking system for three phase utility interface inverters," IEEE Trans. Power Electron., vol. 15, no. 3, pp. 431–438, May 2000.
- [10] M. Karimi-Ghartemani, S. Khajehoddin, P. Jain, A. Bakhshai, and M. Mojiri, "Addressing DC component in PLL and notch filter algorithms," IEEE Trans. Power Electron., vol. 27, no. 1, pp. 78–86, Jan. 2012.
- [11] L. Czarnecki, "On some misinterpretations of the instantaneous reactive power p-q theory," IEEE Trans. Power Electron., vol. 19, no. 3, pp. 828–836, May 2004.